Studies of Anomalous Ionization*

Edgar Y. Choueiri†
Electric Propulsion and Plasma Dynamics Laboratory (EPPDyL)
Princeton University, Princeton NJ 08544.

Hideo Okuda
Princeton Plasma Physics Lab.,
Princeton University
Princeton, NJ. 08544

AIAA Paper: AIAA-94-2465‡

Abstract

In order to improve the accuracy of numerical models of plasma thrusters, a proper representation of the ionization sink is required beyond the current understanding. There are indications that in many plasma thrusters (e.g. MPD and SPT) the ionization is strongly tied to the role of plasma instabilities through electron distributions having suprathermal tails produced by the instabilities and strongly affecting the ionization. Due to the length scales involved in such an "anomalous" or "collective" ionization, the related yet to be understood fundamental phenomena are best studied by staging active gas-plasma interactions using gas injection from an orbiting spacecraft. In this paper, we focus on the interpretation of such an experiment using plasma particle simulation (PIC codes). The goal here is to gain insight into the basic aspects of anomalous ionization. For this purpose, a 2-1/2-D particle simulation model has been developed in order to study neutral gas release experiments into the ionosphere from a satellite. The electrons are assumed guiding center particles while the full dynamics of the ions (with real masses) are followed in time and space. Ionization processes of the neutral gas including charge exchange and electron impact are included by means of the Monte Carlo technique. The model was applied to study the critical ionization velocity (CIV) tests recently conducted as part of the Atlas-1 xenon gas releases from the the space shuttle. The simulation results show how suprathermal electrons produced by a beam instability of the lower hybrid mode, create, through electron impact, a xenon ion population that exceeds that produced by classical (thermal) means, indicating the prevalence of a CIV-type mechanism.

1 Introduction

Ionization represents a largely irrecoverable energy sink in plasma thrusters such as the magnetoplasmadynamic (MPD) thruster. This is mostly due to the fact that, for typical temperatures and pressures of most plasma thrusters, the plasma flow through the chamber is essentially "frozen" with respect to recombination. Most recently, (1992) Randolph et. al. reported the results of a detailed spectroscopic study of ionization[1]. In that study, the ionization front was observed and its thickness measured at a few millimeters which was shown to be 1 to 3 orders of magnitude smaller than what would be consistent with a Maxwellian electron distribution. This and other similar observations hint to the fact that ionization may strongly be tied to the role of plasma instabilities through electron distributions having suprathermal tails produced by the instabilities and strongly enhancing electron impact ionization. This collective or turbulence-driven ionization is sometimes referred to as "anomalous" and in many instances relies on a threshold reached by the relative drift velocity driving the instabilities, hence the name "critical ionization velocity" (CIV) mechanism.

*This work is supported by a grant from the Air Force Office of Scientific Research (AFOSR Grant No. F49620-93-1-0222).

†Member AIAA.

‡Presented at the 25th AIAA Plasma Dynamics and Lasers Conference, Colorado Springs, CO, June 20-23, 1994.

One obstacle in studying the CIV phenomenon experimentally within plasma thrusters is the smallness of the ionization front (about 1 mm thick[1]) and its location (near the gas inlet) which render the ionization region very difficult for access by standard probing techniques.

The importance of the Earth ionosphere and magnetosphere as an ideal laboratory to test the CIV phenomenon has been widely recognized in the past ten years[2, 3]. Staging a CIV interaction in space can be an ideal way to study CIV under conditions closest to the scenario in which the phenomenon was first hypothesized by Alfvén. In space, a relative motion between a gas and a plasma can be easily established by releasing a gas from an orbiting spacecraft or rocket whose velocity with respect to the ionospheric plasma exceed V_c. The ionization region can be made to have dimensions much larger than those of the spacecraft. The use of plasma diagnostics onboard satellites and subsatellites could allow for a thorough and parametric test of CIV.

1.1 Motivation

The goals of our studies are to investigate the fundamentals of anomalous ionization using analytical tools, active space experiments and PIC codes and to develop experimentally verified models that would be available for state of the art plasma thruster fluid codes. In a recent paper[4], we presented a model that could be used to link the nonlinear plasma processes (instabilities, turbulent heating of electrons) to the ionization processes in a plasma thruster. That model focused more on the details of the ionization chemistry and less on the plasma physics (wave generation, saturation and particle heating). In the present paper, we turn our attention to these issues. In particular we seek more insight into the fundamental processes at play during anomalous ionization. This we do by using advanced particle in cell (PIC) simulations to interpret gas release experiments staged specifically to study the CIV process.

1.2 Background on Anomalous Ionization

Originally, collective or anomalous ionization was first invoked in the context of the interaction of a neutral gas with a plasma in a magnetic field in laboratory and space plasma situations. Under certain conditions, a neutral gas undergoes a rapid ionization leading to creation of a highly ionized gas. The process, called the critical ionization velocity (CIV), was proposed by Alfvén[5] and is essentially an instability-driven ionization mechanism where neutral gas is ionized in a more abrupt and efficient manner than can be accounted for by classical means (thermal electron impact, photoionization, charge stripping, charge exchange, etc...). Moreover ionization through the CIV happens in a threshold fashion when a free relative kinetic energy source corresponding to motion perpendicular to the magnetic field in the system exceeds the ionization potential of the neutrals. A critical velocity for anomalous ionization was therefore hypothesized by Alfvén to exist at

$$V_c = (2e\phi_{\text{ion}}/M_n)^{1/2} \tag{1}$$

Here e is the magnitude of the electronic charge, ϕ_{ion} is the ionization potential, and M_n is the mass of a neutral particle.

Theoretical studies and observations of staged CIV interactions in the laboratory have characterized the phenomenon as one in which the free energy source associated with the directed kinetic energy of the relative motion between two plasma components excites plasma microinstabilities of the streaming (or beam) type. These instabilities would then channel a substantial part of the relative kinetic energy to heat electrons preferentially creating a substantial population of electrons with energies above ϵ_i, which would then contribute to a substantially enhanced ionization process. The energy going into ionization ultimately comes from the relative motion (i.e. the beam kinetic energy) and consequently the CIV interaction results in slowing down the relative velocity to near V_c during the interaction.

The instability, typically of the lower hybrid mode, is originally ignited by the cross-streaming of "seed" charged particles in the neutral gas with respect to plasma particles and maintained through the cross-streaming between newly created and old charged particle populations. The lower hybrid wave can easily be destabilized by an ion beam perpendicular to magnetic field when the beam velocity is above the ion thermal speed. It must be emphasized that in all CIV scenarios a "seed" of charged particle must initially exist in the neutral gas. Such seeds could be due to any weak ionization of photonic or thermal origin and, most likely in the case of releases in space, charge exchange collisions.

The CIV phenomenon is of direct relevance to many problems of plasma dynamics where a plasma and a neutral gas are in relative motion and where ionization is a sizable energy sink. Plasma prob-

lems where CIV is believed to play an important role include, interaction of spacecraft exhaust with the ionosphere, plasma guns, plasma thrusters and accelerators, spacecraft environment effects on spacecraft charging and other more natural occurrences in space plasmas such as cometary coma and comet tail formation. Theory, simulation, laboratory and space experiments related to CIV have been recently reviewed extensively by Brenning in ref. [6] .

A few laboratory experiments have been conducted to study the CIV interactions but their results cannot be easily scaled to space plasma problems where the density and magnetic field are, up to a factor of 10^{10} and 10^6 respectively, lower than in the laboratory. Other problems facing laboratory investigations of CIV are the presence of walls or electrodes and the smallness of the ionization front which render the ionization region difficult for access by standard probing techniques.

There has been a few neutral gas injections in the ionosphere to study CIV using shaped charges released from sounding rockets[7]. In these rocket experiments the plasma yield was typically small and difficult to relate conclusively to CIV effects. The following two reasons for the low ionization yield of these experiments have been proposed in the literature: inefficient ion seeding of the neutral gas[8] (due to low rate of charge exchange collisions[9]) and the shortness of the interaction time scale which would produce small yields even if CIV was operative[7].

Neutral gas releases from orbiting spacecraft are more promising than rocket experiments for studying the parametric dependencies of a CIV interaction since they allow the experiments to be repeated under various conditions.

1.3 Recent CIV tests in Space

We are involved in modelling two recent space-based studies of anomalous ionization. The first experiment was a series of releases conducted from the Russian scientific satellite APEX in 1992 and 1993. Data from the various plasma diagnostics on APEX have just recently been reduced and will be presented in [10]. In the present paper, we consider the currently more documented CIV tests that were made as part of the ATLAS-1 experiments conducted on the shuttle orbiter Atlantis on March 24, 1992. The neutral xenon releases on ATLAS-1 were shown in ref. [11] to satisfy many of the criteria thought to be necessary for a positive CIV test[12] and had the important advantage of a high mass flow rates (1.5 moles/sec) which is also critical for producing enough ion seeds through charge exchange[9].

The ATLAS-1 releases showed a factor of 60 increase in plasma density following each of the 100 msec long neutral xenon releases[11]. Wave activity in the lower hybrid band during the releases was also reported[13].

The study of the ATLAS-1 tests can be enhanced by applying advanced numerical simulation codes that can handle realistic conditions of the experiments. In this paper, we discuss a numerical simulation model developed specifically to study such neutral gas releases in the ionosphere. We present simulation results obtained by applying the code to the ATLAS-1 CIV tests using realistic parameters reported in ref. [11].

2 Previous Numerical Simulations

Since 1984, particle-in-cell (PIC) codes have been used in the study of the CIV effect. The PIC simulations to date have clarified many aspects of the CIV effects including: the threshold aspect of the interaction[14], suprathermal electron production[15], the role of electromagnetic effects[16], the presence of ionization fronts[17], the importance of elastic scattering and the atomic physics such as charge exchange, excitation and ionization from metastable states[9, 18] and the importance of initial ion seed in the neutral gas[8].

Most of the simulations have been one-dimensional except for those in ref. [16, 17] in which two-dimensional simulations with artificial mass ratios were carried out using a small grid. Consequently, until now the simulations have been concerned with the investigation of fundamental aspects of CIV and were not directly applied to any specific gas release experiment in space.

In order to model neutral gas releases in the ionosphere under realistic conditions we use a 2&1/2-dimensional PIC code that can handle real mass ratios and realistic spatial extensions. The effects included in the model are listed in Table 1 for comparison with those of previous simulation models. The present model neglects electromagnetic effects since these were shown not to be important for the CIV interaction when[16]

$$V < (1 + \beta_e)^{1/2} v_A \tag{2}$$

(where V is the relative velocity, β_e the electron beta

Reference	[14]	[15]	[19]	[16]	[17]	[9]	[18]	[8]	This work
Year	84	85	86	88	88	90	90	92	94
Dimensions	1-D	1-D	1-D	2-1/2-D	2-1/2-D	1-D	1-D	1-D	2-1/2-D
EM effects				√	√				
e^--impact ioniz.	√		√	√	√	√	√	√	√
Charge X. Coll.			√	√	√	√	√	√	√
e^--impact excit.			√	√	√	√	√		
Elastic Scat.			√	√	√	√	√	√	
Real Dimensions									√
Real m_i/m_e								√	√

Table 1: Chronological list (1984-1994) of referenced PIC simulation models used for CIV studies and the effects considered by each. The effects are, dimensionality, electromagnetic effects, ionizing, charge exchange, excitation and elastic collisions, real spatial dimensions and real mass ratios.

and v_A the Alfvén velocity) a condition amply satisfied in most ionospheric release experiments. Although various collisional processes can be easily included and handled by the code we limit the simulations discussed here to include only the most important ones, namely ionizing (electron impact) and charge exchange collisions.

3 Simulation Model

Shown in Fig. (1) is a sketch of the particle simulation model developed specifically for studying the neutral gas release experiments into the ionosphere. The model is two-and-one-half-dimensional in which two spatial coordinates, x and y, and three velocity components are followed in time. Full dynamics of the ions are followed in time, while the electrons are treated as guiding center particles, where rapid gyration around the guiding center has been averaged out. This averaging is tolerable for our case because we are not interested in the high frequency electron gyromotion, and it allows us to use a larger integration time step, which is essential for simulations using realistic plasma parameters[20]. The code follows the motion of the background and ionized plasma in a given uniform magnetic field representing the geomagnetic field and a self-consistent electrostatic field. Extension to full three dimensions is straightforward by using higher order interpretations to simulate a large three dimensional volume[20].

Using the Langmuir probe measurements for the ATLAS-1 releases reported in ref. [11] we set the background oxygen ion density at $5 \times 10^4 \mathrm{cm}^{-3}$ and the electron temperature at 0.1 eV. We also set the magnetic field strength at 0.7 gauss and the pitch angle of the velocity vector at 81 degrees as was the case for the actual releases. Main components of the background neutral gases are O and N_2 whose densities are $10^7 - 10^8/\mathrm{cm}^3$. The Debye length is typically 1 cm and the electron plasma and gyrofrequencies are about 10^7/s. The oxygen ion plasma frequency which is close to the lower hybrid frequency is about equal to 5.8 x 10^4/s.

The mass flow rate of 1.5 moles/s of the ATLAS-1 releases, which lasted 100 msec each, is equivalent to 10^{23} particles for a typical release. The reported observations suggest that a rapid ionization took place within a few ms[11].

The interaction of the neutral xenon gas with the background plasma is treated by means of the Monte-Carlo technique[21] including charge exchange

$$X_e + O^+ = X_e^+ + \mathrm{O}$$

and electron impact inonization

$$X_e + \mathrm{e} = X_e^+ + 2\mathrm{e}$$

The cross section for the oxygen-xenon charge exchange is $10^{-16}\mathrm{cm}^2$ at 10 eV electron energy and increases to $2\mathrm{x}10^{-15}\mathrm{cm}^2$ at 100 eV[22]. The ionization energy of the ground state xenon atom is 12.13 eV and the dependence of the cross section for electron impact ionization on the energy is described in ref. [23] and is shown to increase almost linearly from threshold, reaching the maximum of 6.2 x $10^{-16}\mathrm{cm}^2$ at 120 eV then decreasing to about 2 x $10^{-16}\mathrm{cm}^2$ at 1 keV.

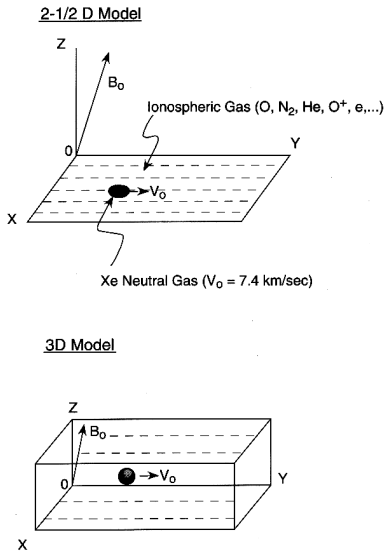

Figure 1: Sketch of the numerical simulation models developed to study neutral gas release experiments into the ionosphere. A two-and-one-half-dimensional model (top) has two spatial coordinates, x and y, and three velocity components. Extension to a three dimensional model (bottom) is straightforward.

In the simulations discussed here, we did not include other binary interactions which could be easily handled by the code. Among such interactions are line excitation, ionization from the (6s) metastable state, which can have cross sections as large as 10^{-14}cm^2 and elastic scattering of the X_e^+ ions by the xenon and oxygen neutral gases. These collisional effects will be included in a future simulation.

The dimensions of the simulation grid, shown in Fig. 1 are set to either $256(x) \times 512(y)$ or $256(x) \times 1024(y)$ which, for our particular case with the Debye length of 1 cm, correspond to either 256 cm $\times$ 512 cm or 256 cm $\times$ 1024 cm in real dimensions after setting the grid size equal to the Debye length.

Since the space shuttle and hence the neutral xenon gas are moving at 7.4 km/s orbital speed in the y direction, our simulation system is therefore traversed in 1.4 ms, unless the system length is stretched in the y direction.

The ATLAS-1 space observations[11] show, however, that a significant enhancement of ionization takes place within that time scale, so that the present simulation is large enough to study at least the initial stage of the interaction.

As mentioned earlier, real mass ratios are used for the electrons, oxygen and xenon ions. The time step of integration used in the simulation was (2 - 5)ω_{pe}^{-1} which corresponds to (2 - 5)x10^{-7} s. While the detailed shape of the xenon gas is not known, we shall assume in our model that it is a sphere with a uniform density moving at the shuttle speed in the ionosphere. Since the xenon gas expansion speed of 61m/s is much lower than the 7.4 Km/s orbital speed, the changes in the radius and the density during the simulation were ignored.

The boundary conditions for the particles and fields are the following. First, the background ionospheric oxygen ions and electrons, which are assumed uniform initially, are assumed periodic. The ionospheric ions, for example, leaving a boundary are inserted back from the opposite boundary. This is roughly equivalent to an assumption of a vast ionospheric background. The xenon ions produced by the impact ionization and charge exchange are assumed lost once they leave the boundary of the simulation. High energy electrons accelerated by the plasma waves are also considered lost once they cross the simulation boundaries. The ideal boundary conditions for the electrostatic potential would be such that the potential vanishes at a point where the distance from the xenon cloud is far enough. This can be approximated by using a sine Fourier transform for the system which sets the values of the potential at the boundary zero. As the waves grow to large amplitude at a later phase of the simulation, however, the plasma waves reach the boundary without much attenuation, so that some of the waves are reflected. In fact, the use of the periodic boundary condition gives results not much different from those that would be obtained using the sine Fourier transform. This is because the largest wave amplitude in the system remains concentrated near the xenon cloud.

In the example given below, we shall assume that the neutral xenon gas has a density of 3×10^{14}/cm^3 with its radius of 8 cm. This would corresponds to an early phase of the gas release.

The resulting evolution of the beam instability, the formation of suprathermal tails, the wave emission and the enhancement to ionization under the above listed conditions are described by the simulation results in the next section.

4 Simulation Results

The released xenon neutrals have effectively the spacecraft orbital velocity of 7.4 km/s, and can undergo charge exchange with the background oxygen ions, resulting in an energetic xenon ion beam. Such an xenon ion beam is able to excite plasma waves near the oxygen lower hybrid and ion cyclotron waves propagating nearly perpendicular to the magnetic field. The lower hybrid and ion cyclotron waves, in turn, accelerate xenon ions perpendicular to magnetic field and electrons along magnetic field at roughly the same rate[24]. The energetic electrons in turn can enhance ionization of the xenon neutral gas so that the original streaming energy of the neutral xenon is channeled through the waves to the ionization. The coupling of the lower hybrid wave to ions and electrons is comparable at an angle of propagation given by $k_{||}/k_{\perp} = (m_e/m_i)^{1/2}$. If the angle is larger than this value, more energy is fed into the electrons thus enhancing ionization. The threshold ion beam velocity, however, also increases with this angle[24]. This picture is upheld by the following simulation results.

Shown in Fig. (2) are the results of the simulations at t = 1000 ω_{pe}^{-1} which corresponds to approximately 0.1 ms. The electrostatic contour plot shown in panel (a) indicates a presence of potential fluctuations near the xenon cloud caused by the newly born xenon ions through charge exchange. Since the neutral xenon density is high, the rate at which the xenon ions is created is substantial. The rate is given by $\sigma_c n_{O^+} n_{X_e} V_r$, so that at t = 1 ms the xenon density becomes comparable to the oxygen density near the xenon cloud. The potential fluctuations arise from the high speed xenon ions moving through the ionosphere. Here V_r is the relative speed between the neutral xenon gas and the oxygen ions.

Shown in panel (b) of Fig. (2) is the location of the xenon cloud moving at a speed of 7.4 km/s. As mentioned earlier, the cloud remains unchanged on the time scale of the simulation. A scatter plot of the electron spatial distribution are shown in panel (c), which indicates that it is essentially uniform at this time. The average electron density shown in panel (d), however, indicates significant perturbations at the center of the system where the xenon cloud is located. This perturbation is created by the newly born xenon ions trying to maintain the charge neutrality. The xenon ions are moving at high speed so that they tend to generate charges at the boundary, generating density perturbations as well as potential fluctuations shown in panels (a) and (d).

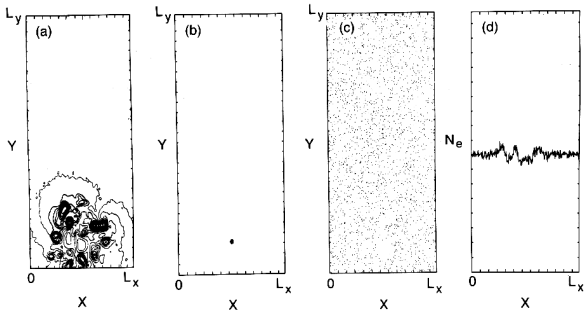

Figure 2: Simulation results for a neutral gas cloud with a density of $3x10^{14}/cm^3$ and a radius of 8 cm at $t = 0.1$ ms. Shown in the Figure are electrostatic potential contours (a), location of the neutral xenon gas in the (x, y) plane (b), scatter plot of the ionospheric electrons (c) and the electron density averaged over y-direction (panel d). At this early time of the simulation, the charge exchange process between the xenon neutral gas and the ionospheric oxygen ions produced a small number of xenon ions generating potential fluctuations near the xenon cloud. Local density perturbations can also be seen in panel (d).

Shown in Fig. (3) are the corresponding distributions for the electron velocity (a), the oxygen ion perpendicular velocity (V_x) (b), xenon ion perpendicular velocity (V_x), (c), and (V_y) , (d) components. Since the time is still short for the lower hybrid waves to grow, electrons and oxygen ions are essentially the same as the initial ionospheric distributions at 0.1 eV. The xenon ions produced by the charge exchange processes are streaming at the orbital speed. Note that the velocities shown in Fig. (3) are normalized with respect to the thermal velocity at the ionospheric temperature.

Shown in Fig. Fig. (4) are the results of the simulations at t = 4 ms for scatter plots for the xenon neutral gas (a), scatter plot for thr xenon ions (b), and newly created electrons (c) produced by electron impact ionization. The xenon neutral cloud has moved further across the magnetic field. The xenon ions also move with the orbital speed, together with the xenon neutral gas. The xenon ions, however, spread radially as they gyrate out from within the cloud. The newly created electrons spread out rapidly as seen in panel (c) of Fig. (4) owing to their large mobility. The charge neutrality is maintained by the background ionospheric oxygen ions and electrons, whose densities are much higher than the newly born electrons

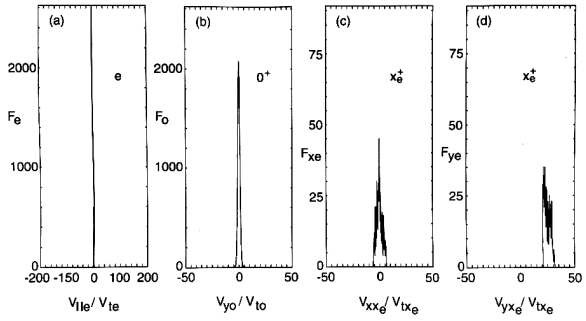

Figure 3: Results of the same simulation as in Fig. (2), showing distributions for the electron velocity along magnetic field (a), the oxygen ion perpendicular velocity V_y (b), the xenon ion perpendicular velocity V_x (c), and the associated V_y component (d). Both the electrons and oxygen ions remain the same as the initial ionospheric distributions, while the xenon beam ions are created through charge exchange. Note that the velocities are normalized by the thermal velocities of the corresponding species at the ionospheric temperature, 0.1 eV.

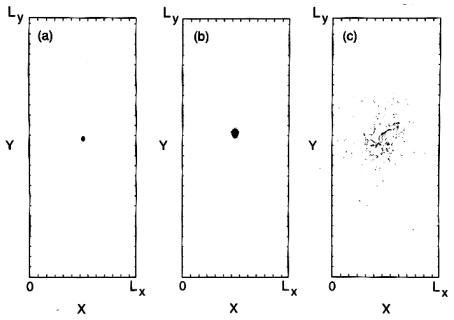

Figure 4: Results for the location of the xenon neutral gas (a), scatter plots for the xenon ions (b), and for the newly created electrons (c) produced by electron impact ionization. Note the xenon ions move with the xenon neutral gas as expected except for radial expansion as shown in panel (b). The newly created electrons, on the other hand, spread out quickly from the neutral gas. Charge neutrality is maintained by the ionospheric oxygen ions and electrons.

at this time. We note that at this time the number of the xenon ions produced by charge exchange is much larger than the electron impact produced xenon ions (the ratio is 100 to 1). This is because there are very few high energy electrons produced at this time.

Shown in Fig. (5) are the corresponding velocity distributions for the electrons (a), oxygen ions (b), and xenon ions (c) at this time (0.4 ms). It is clear that both the electrons and oxygen ions are accelerated somewhat from their initial ionospheric distributions, which are also included in panels (a) and (b). The xenon ion beam plotted in panel (c) shows a slowing down from the orbital speed, and, at the same time, a spreading caused by velocity space diffusion. The acceleration and diffusion of the particles are caused by plasma instabilities near the lower hybrid waves. The energy lost by the xenon ion beam is channeled to the acceleration of the electrons, which can, in turn, enhance the ionization of the neutral xenon gas substantially as the suprathermal electron population increases.

Shown in Fig. (6) is the power spectrum for a Fourier mode, $(m, n) = (4, 3)$, (a), and the spectrum measured at a location near the xenon neutral cloud, (b). It is clearly seen that both spectra have a peak frequency near 2 ω_{po} which is close to the lower hybrid frequency including the electron response[24]. This is a direct evidence for the excitation of the oxygen lower hybrid waves by the xenon beam generated by the charge exchange process. The electrons accelerated by the lower hybrid waves, in turn, should increase the impact ionization leading to further enhancement of the instability and a self-sustaining collective ionization process.

Shown in Fig. (7) are the results of the simulation at t = 0.7 ms. The spatial distribution of xenon ions produced by electron impact ionization is shown in panel (a). Note that the cloud expands radially as it moves with the shuttle orbital velocity. It is interesting to note that the center of the cloud has much higher density surrounded by the outer region at lower density. This is clearly shown in panel (b) where the average xenon ion density is shown as a function of x. The peak xenon ion density is located near the center of the xenon neutral cloud, and its density is a quarter of the ambient oxygen ion density. At this time the number of xenon ions produced by the electron impact exceeds the number of xenon ions produced through charge exchange with ionospheric ions. More on this point will be said later.

The electron velocity distribution is shown in panel (c) of the same figure at t = 0.7 ms together with the initial ionospheric electron distribution. It is clear that the tail electrons are much hotter now, with a substantial portion having energies as high as

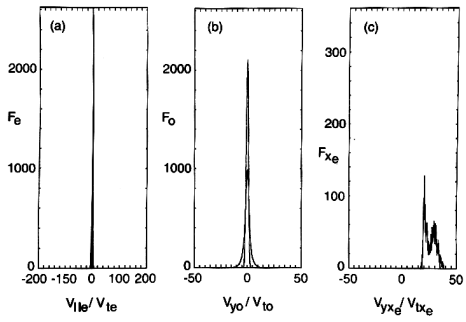

Figure 5: The velocity distributions for the electrons (a), oxygen ions (b), and xenon ions (c) at t = 0.4 ms. It is shown that acceleration of the electrons along and oxygen ions across the magnetic field began to take place as a result of the plasma instability near the oxygen lower hybrid waves. The delta-function-like distributions in panels (a) and (b) correspond to the initial electron and oxygen ion distributions at the ionospheric temperature.

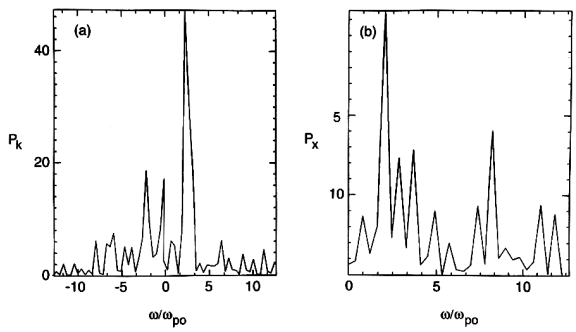

Figure 6: Power spectra of the charge density for a Fourier mode $(m, n) = (4, 3)$ (a), and at a location near the neutral gas in the (x, y) plane (b). Note for both cases, a peak near 2 ω_{po} is clearly seen, which corresponds to the oxygen lower hybrid wave.

20 eV. Such electrons can indeed enhance the impact ionization of the neutral xenon gas because of both the enhanced density of electrons above the ionization threshold and the increase in the ionization cross section at these higher energies. The xenon ion V_y velocity distribution produced by the impact ionization is shown in panel (d). The drift speed is substantially smaller than the orbital speed, suggesting that the xenon kinetic energy associated with the orbital motion is channeled to the ionization as well as to the acceleration of various kind of particles.

At t = 1 ms, as shown in Fig. (8), the heating of the electrons and ionization of the xenon gas happen at a faster rate. The energy distribution of the electrons shown in panel (a) indicates a further suprathermal tail enhancement, with a substantial portion of the electrons having energies as high as 60 eV. The ionoshperic oxygen ions shown in panel (b) is also heated substantially. The xenon ions produced by the impact ionization shown in panel (c) and by the charge exchange shown in panel (d) are accelerated and at the same time their drift speed have decreased significantly. Note that the number of xenon ions produced by impact ionization is larger than the number of xenon ions produced through charge exchange by a factor of 3 at this time.

Shown in Fig. (9) is the time record of the xenon ions produced through charge exchange (open circles) and by electron impact ionization (solid circles). It is clear that the impact ionization, once it is triggered, increases much more rapidly than the charge exchange ionization which is more or less linear in time. Since the impact ionization depends on the high energy electron population, it is essential to accurately follow the development of the electron distribution by means of self-consistent means such as by the PIC simulation reported in this work. The electron impact ionization completely dominates over charge exchange ionization after a few hundred microseconds into the simulation demonstrating that an anomalous process such as CIV could indeed be important during neutral gas release experiments in space, in general, and the ATLAS-1 xenon releases, in particular.

5 Concluding Remarks

We have used a particle simulation model to study the fundamentals of anomalous ionization and gain insight into the character of the wave generation, particle heating, diffusion and enhanced plasma production that accompany this type of ionization.

The model was applied to the xenon gas release experiments conducted during the ATLAS-1 mission. The model still does not include all the subsidiary binary reactions (line excitation and radiation, elastic collisions, stripping ionization and multiple ionization) which will be added in future simulations. It has shown, however, how xenon ions, created from the released gas through charge exchange with ionospheric ions, and streaming with a velocity exceeding V_c, can

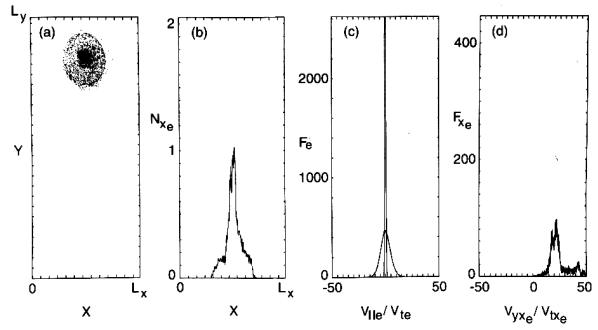

Figure 7: Results of the simulation at t = 0.7 ms for the xenon ion cloud produced by the electron impact in the (x, y) space (a), its average density in x (b), the electron velocity distribution (c), and the xenon ion velocity distribution (d).

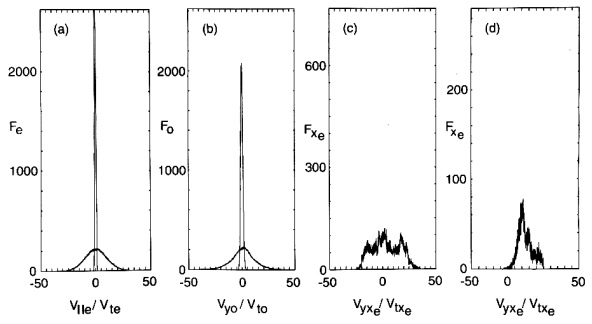

Figure 8: Results of the simulation at t = 1 ms for the velocity distributions of the electrons (a), oxygen ions (b), electron impact produced xenon ions (c), and charge exchange produced xenon ions (d).

drive plasma waves near the lower hybrid frequency unstable, which can produce suprathermal electrons that can, in turn, lead to a rapid ionization of the neutral gas. This is essentially the CIV effect.

The number of xenon ions produced through the collective (CIV) effect (i.e. by impact with suprathermal electrons accelerated by the waves) increases much more rapidly than the number of ions created through classical charge exchange ionization. This is in contrast with the finding in ref. [25], where a quenching of the CIV effect was expected to happen when the CIV ionization rate becomes comparable with the charge exchange rate. The reason for this discrepancy may well be due to the neglect of the growing nonlinear effects in the quasi-linear analysis

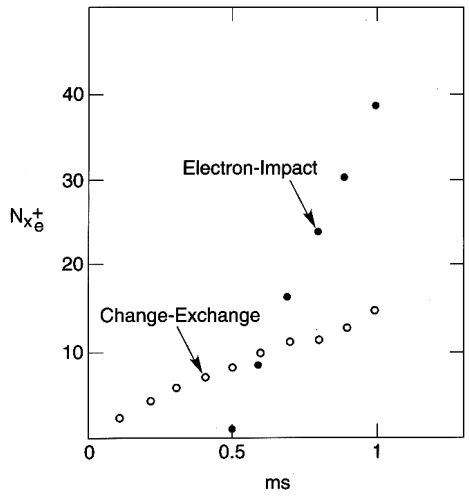

Figure 9: Time record for the charge exchange produced xenon ions (open circles) and electron impact produced xenon ions (solid circles). The average xenon ion density is normalized by the average ionospheric plasma density, assuming that the total xenon ions are confined within the initial xenon neutral cloud. It is shown that the ionization produced xenon ions obtained a density as much as 30 times of the background oxygen ion density if there were no xenon ion diffusion in space. As discussed in the text, xenon ions actually diffused out radially, reducing its density comparable to the oxygen ion density at t = 1 ms.

of that work, as suspected by the authors themselves.

While our numerical simulation followed the evolution of the xenon gas release only to about 1 ms time, the total number density of the xenon ions produced by CIV and charge exchange becomes already comparable to the density of the ionospheric oxygen ions. With longer simulations we expect the xenon ions produced through the CIV effect to keep on increasing rapidly so that their density can far exceed the oxygen ion density within a relatively short period of time.

Since we found that, for the ATLAS-1 release conditions, CIV ionization dominates over charge exchange after only a short time (a few hundred microseconds), and since the observations show an increase of the density of a factor of 60 a few milliseconds into the release[11], it seems likely that this density enhancement can be attributed to the CIV effect. This would be ascertained more quantitatively when all the relevant subsidiary reactions are included in

the model.

The findings described above concerning the nonlinear evolution of wave generation and particle heating during anomalous ionization, will be instrumental in the further development of our model of anomalous ionization in plasma thrusters[4]. By combining the detailed ionization chemistry of that model and the nonlinear plasma physics revealed in the present study, we hope to arrive at a realistic model that can be used to improve the realism of plasma fluid codes of plasma thrusters.

Acknowledgments. The authors would like to thank Dr. Shu T. Lai and Dr. Jill Marshall for stimulating discussions and useful information.

References

[1] T.M. Randolph, W.F. Von Jaskowsky, A. J. Kelly, and R. G. Jahn. Measurement of ionization levels in the interelectrode region of an MPD thruster. In 28^{th} *Joint Propulsion Conference*, Nashville, TN, 1992. AIAA-92-3460.

[2] E. Möbius, R.W. Boswell, A. Piel, and D. Henry. A Spacelab experiment on the critical ionization velocity. *Geophysical Research Letters*, 6:29–31, 1979.

[3] I. Axnäs. Some necessary conditions for a critical velocity interaction between the ionospheric plasma and a xenon cloud. *Geophysical Research Letters*, 7:933–936, 1980.

[4] E.Y. Choueiri. Anomalous ionization in the MPD thruster. In 23*rd International Electric Propulsion Conference*, Seattle, WA, USA, 1993. IEPC-93-067.

[5] H. Alfvén. Collision between a nonionized gas and a magnetized plasma. *Review of Modern Physics*, 32(4):710–713, 1960.

[6] N. Brenning. Review of the CIV phenomenon. *Space Science Reviews*, 59:209–314, 1992.

[7] R.B. Torbert. Review of critical velocity experiments in the ionosphere. *Advances in Space Research*, 10:47–58, 1990.

[8] R.J. Biasca. *Numerical Simulation of the Crirical Ionization Velocity Mechanism*. PhD thesis, Massachusetts Institute of Technology, Cambridge, MA, USA, 1992.

[9] J.D. Person, H. Resendes, and D. Hastings. Effects of collisional processes on the critical ionization velocity hypothesis. *Journal of Geophysical Research*, 95:4039, 1990.

[10] V. Dokukin, A. Volokitin, Y. Ruzhin, V. Oraevksy, and E.Y. Choueiri, 1994. CIV Tests on APEX. COSPAR Meeting, Hamburg, Germany. July, 1994.

[11] J.A. Marshall, J.L. Burch, E.Y. Choueiri, and N. Kawashima. CIV experiments on ATLAS-1. *Geophysical Research Letters*, 20(6):499–502, 1993.

[12] S.T. Lai and E. Murad. Inequality conditions for critical velocity ionization space experiments. *IEEE Transactions on Plasma Science*, 20:770–777, 1992.

[13] E.Y. Choueiri, J.A. Marshall, J.L. Burch, H. Okuda, and N. Kawashima. Collective plasma phenomena observed during the CIV tests on ATLAS-1. In *1993 Spring Meeting of the American Geophysical Union*, page 233, San Baltimore, CA, 1993. SA51C-10.

[14] S. Machida, T. Abe, and T. Terasawa. Computer simulation of critical ionization velocity. *The Physics of Fluids*, 27:1928, 1984.

[15] T. Abe and S. Machida. Production of high energy electrons caused by counterstreaming ion beams in an external magnetic field. *The Physics of Fluids*, 28:1178, 1985.

[16] S. Machida and C. Goertz. The electromagnetic effect on the critical ionization velocity. *Journal of Geophysical Research*, 93:11495, 1988.

[17] S. Machida, C. Goertz, and G. Lu. Simulation study of the ionizing front in the critical ionization velocity phenomenon. *Journal of Geomagnetism and Geoelectricity*, 40:1205, 1988.

[18] W. McNeil, S. Lai, and E. Murad. Interplay between collective and collisional processes in critical velocity ionization. *Journal of Geophysical Research*, 95:10345, 1990.

[19] S. Machida and C. Goertz. A simulation study of the critical ionization velocity process. *Journal of Geophysical Research*, 91:11965, 1986.

[20] W.W. Lee and H. Okuda. A simulation model for studying low frequency microinstabilities. *Journal of Computational Physics*, 26:139, 1978.

[21] C.K. Birdsall, 1991. IEEE Trans. Plasma Sci. **19**, 65.

[22] M. Matic, V. Sadis, M. Vujovic, and B. Cobic, 1990. J. Phys. B: Atom, Molec. Phys. **13**, 3665.

[23] D. Rapp and P. Englander-Golden. Total cross sections for ionization and attachement in gases by electron impact I. Positive ionization. *Journal of Chemical Physics*, 43(5):1464–1479, 1965.

[24] J.M. Kindel, H. Okuda, and J.M. Dawson, 1972. Phys. Rev. Lett. **29**, 995.

[25] E. Moghaddam-Taaheri and C.K. Goertz. Quasilinear numerical study of the critical ionization velocity effect. *Journal of Geophysical Research*, 98(A2):1443, 1993.